

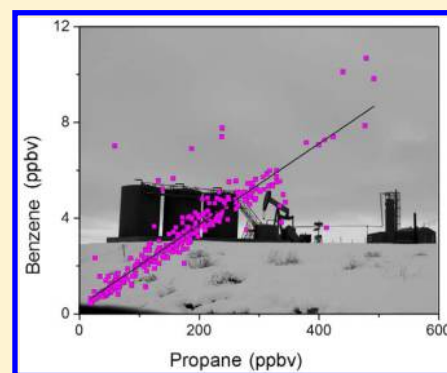
# Highly Elevated Atmospheric Levels of Volatile Organic Compounds in the Uintah Basin, Utah

D. Helmig,\* C. R. Thompson, J. Evans, P. Boylan, J. Hueber, and J.-H. Park

Institute of Arctic and Alpine Research (INSTAAR), University of Colorado, Boulder, Colorado 80309-0450, United States

**S** Supporting Information

**ABSTRACT:** Oil and natural gas production in the Western United States has grown rapidly in recent years, and with this industrial expansion, growing environmental concerns have arisen regarding impacts on water supplies and air quality. Recent studies have revealed highly enhanced atmospheric levels of volatile organic compounds (VOCs) from primary emissions in regions of heavy oil and gas development and associated rapid photochemical production of ozone during winter. Here, we present surface and vertical profile observations of VOC from the Uintah Basin Winter Ozone Studies conducted in January–February of 2012 and 2013. These measurements identify highly elevated levels of atmospheric alkane hydrocarbons with enhanced rates of  $C_2$ – $C_5$  nonmethane hydrocarbon (NMHC) mean mole fractions during temperature inversion events in 2013 at 200–300 times above the regional and seasonal background. Elevated atmospheric NMHC mole fractions coincided with build-up of ambient 1-h ozone to levels exceeding 150 ppbv (parts per billion by volume). The total annual mass flux of  $C_2$ – $C_7$  VOC was estimated at  $194 \pm 56 \times 10^6 \text{ kg yr}^{-1}$ , equivalent to the annual VOC emissions of a fleet of  $\sim 100$  million automobiles. Total annual fugitive emission of the aromatic compounds benzene and toluene, considered air toxics, were estimated at  $1.6 \pm 0.4 \times 10^6$  and  $2.0 \pm 0.5 \times 10^6 \text{ kg yr}^{-1}$ , respectively. These observations reveal a strong causal link between oil and gas emissions, accumulation of air toxics, and significant production of ozone in the atmospheric surface layer.



## INTRODUCTION

Tropospheric ozone is a secondary air pollutant produced photochemically through complex reactions involving volatile organic compounds (VOCs) and nitrogen oxides ( $\text{NO}_x$ ).<sup>1</sup> The current EPA National Ambient Air Quality Standard (NAAQS) for 8-h average ozone levels is 75 ppbv (parts per billion by volume, i.e.,  $\text{nmol mol}^{-1}$ ). Levels above this threshold are considered to be harmful to human health, and high levels of ozone are known to cause respiratory distress and be responsible for an estimated 5000 premature deaths in the U.S. per year.<sup>2</sup> Because of the photochemical nature of ozone production, tropospheric ozone pollution has traditionally been considered an urban, summertime phenomenon; thus, the discovery of rapid, photochemical ozone production during the winter months in 2008 in the Green River Basin of Wyoming was unexpected.<sup>3,4</sup> Since that time, high wintertime ozone has also been discovered in the Uintah Basin in northeastern Utah.<sup>5,6</sup> These two regions are similar in that they are both topographic basins, they are predominantly rural (Uintah County is home to  $\sim 30,000$  people), and they are home to two of the highest producing oil and gas fields in the United States. Currently, the Uintah Basin has approximately 4300 oil and 6900 gas producing wells in operation, with proposals in place for nearly 25,000 more.

Elevated ambient air ozone levels were first reported in the Uintah Basin in the winter of 2009/2010 at Ouray in the center of the Basin. Follow-up measurements from an expanding

network of ozone monitoring stations have since shown a preponderance of high ozone conditions, with ozone levels exceeding the 8-h NAAQS at all stations located inside the Basin, and with the number of exceedences reaching up to 39 days at individual monitoring stations (Ouray, winter of 2013), and 1- and 8-h ozone maxima in the Uintah Basin exceeding those reported for recent years for summertime values from the Los Angeles Basin.<sup>7</sup> Here, we report findings from the 2012 and 2013 Uintah Basin Winter Ozone Studies (UBWOS), which aimed at elucidating the causes for the wintertime ozone production events seen in this region.

## METHOD DESCRIPTION

Experiments reported here were conducted at the Horse Pool site, at  $40.14^\circ\text{N}$ ,  $109.47^\circ\text{W}$ , 1530 m asl. This site is on the northern edge of the most extensive gas field in the Basin, with  $\sim 160$  well pads surrounding the site within a 5 km radius (Figure 1). Continuous measurements of ozone, methane, and a suite of nonmethane hydrocarbons (NMHCs) were conducted from January 30 through February 26, 2012, and from January 25 through February 19, 2013, from sampling inlets located on a 2-m tower and on a tethered balloon. The

Received: November 12, 2013

Revised: February 25, 2014

Accepted: March 13, 2014

Published: March 13, 2014

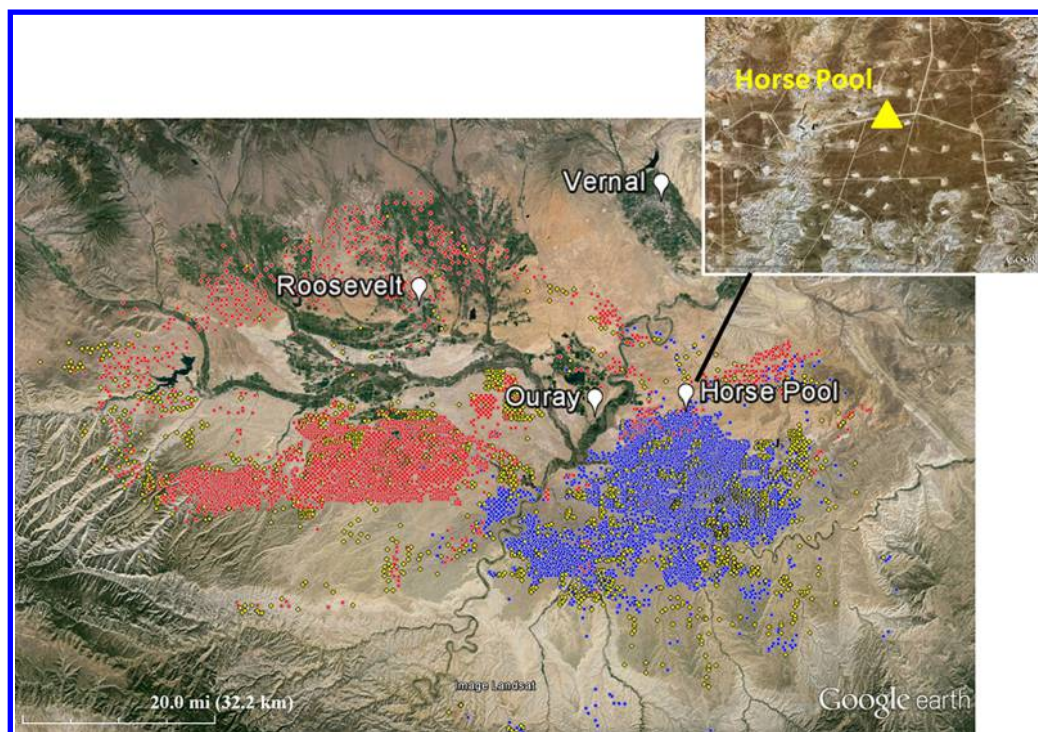


**Figure 1.** Location of the Horse Pool study site in the Uintah Basin, in northeast Utah, USA, with reported oil (red) and gas (blue) producing wells and yellow markers showing wells under development (end of 2012). The Horse Pool site, shown by the yellow triangle in the inset, is located at the northern edge of the gas production area in the eastern part of the Basin. The five closest active wells were at approximate distances of 291, 311, 498, 516, 567, and 621 m.

vertical profiling used a stationary 20-foot diameter Sky-Doc balloon for raising three long sampling lines that delivered air to monitors in a mobile laboratory near the balloon winch (Supporting Information, Figure 1). Each sampling line was made of thin-wall, black Teflon of 0.78 cm o.d., 0.64 cm i.d., and  $\sim 190$  m length. Lines were thoroughly cleaned, conditioned with elevated ozone (24 h at 300 ppbv), and repeatedly tested for compound recoveries prior to and during the field campaign, with recoveries for all reported species of  $>95\%$ . Sampling inlets were made of AcroDisc, 50 mm diameter glass fiber inlet filters (Pall Corporation, Port Washington, NY) and air was drawn through these lines continuously at  $\sim 4$  L  $\text{min}^{-1}$  with individual monitors then pulling a fraction from this flow for the respective gas measurements inside the trailer. Inlets were attached to a secondary balloon tether line and raised with the SkyDoc to heights above ground of  $\sim 51$ , 102, and 153 m. Surface-level measurements were made by sampling from a fourth inlet at 2 m above the ground from a tower  $\sim 12$  m south of the trailer. All sampling line measurements were intercompared and corrected for small line and instrument biases ( $<5\%$ ) by once daily running all inlets side by side on the tower. Ozone measurements were conducted continuously from each line at 1 min time resolution using a total of five UV absorption ozone monitors (one Thermo Environmental (TEI) Corp. Model 49i, one TEI Model 49, one Advanced Pollution Instrumentation Inc. (API) Model 400, and two MonitorLabs Model 8810). These monitors were calibrated against a reference transfer standard that was calibrated against a reference standard at the NOAA-Global Monitoring Division, Earth System Research Laboratory in Boulder, CO. Accuracy and precision of the ozone measurements are estimated at 1 ppbv (respectively 1%  $> 100$  ppbv) and 0.5 ppbv for 1-min data, respectively. Other

gases were analyzed with one dedicated monitor by sequentially connecting the sampling flow path to one of the four inlet lines using valves and a manifold. Methane was measured at 3 min time resolution with a gas chromatograph (GC)–flame ionization detector (FID) Methane Analyzer (Baseline, Lyons, CO), which was calibrated using a 1.03 ppmv (parts per million by volume, i.e.,  $\mu\text{mol mol}^{-1}$ ) gravimetric standard (Scott-Marrin Inc., Riverside, CA). The uncertainty of the methane measurement was estimated at 0.8%, derived from the uncertainty in the standard (0.01%), and the measured mean precision of standard measurements (0.8%). NMHCs were analyzed in the sample stream by gas chromatography after directing the sample stream through a sodium thiosulfate-coated glass fiber filter for removal of ozone. A GC with a Peltier-cooled microadsorbent trap for sample pre-focusing, followed by thermal desorption and temperature-programmed separation with FID, was operated at the site. This instrument is similar to the one described in Tanner et al. in 2006.<sup>8</sup> It was configured for analysis of  $\text{C}_2$ – $\text{C}_{10}$  VOC with a sample collected every  $\sim 30$  min over a 6-min sampling time. Quantified compounds were those listed in Table 1, which together made for  $>85\%$  of the observed VOC peak area. Whole air samples were also collected over a  $\sim 2$ -min sampling time in programmable flask packages (PFP, Atmospheric Observing Systems, Boulder, CO) for later analysis on two different laboratory GCs with similar sample preconcentration techniques, with one of the instruments equipped with an FID and the other one operating with a mass spectrometer and FID detector after splitting the column flow. The GC-FID instrument is of the same configuration as the one used in the Global VOC Monitoring Program.<sup>9</sup> A series of five gravimetric and ambient air calibration standards were used for the GC response factor determination (see the Supporting

**Table 1. Molar and Mass Ratios of NMHC/Methane from All Combined 2012 and 2013 Surface Measurements and Estimated Annual NMHC Flux**

compound	molar NMHC/CH <sub>4</sub> ratio <sup>a</sup>	mass NMHC/CH <sub>4</sub> ratio	annual flux <sup>b</sup> 10 <sup>6</sup> kg yr <sup>-1</sup>
ethane	0.063	0.14	65
propane	0.031	0.097	47
iso-butane	0.0061	0.025	12
<i>n</i> -butane	0.0089	0.037	18
iso-pentane	0.0042	0.022	10
<i>n</i> -pentane	0.0032	0.017	8.0
<i>n</i> -hexane	0.0018	0.011	5.4
benzene	0.00058	0.0032	1.6
toluene	0.00064	0.0042	2.0
Σ minor NMHC <sup>c</sup>		0.053	25
total		0.40	194

<sup>a</sup> The ratios in column 2 reflect the correlation results as shown in the examples in Figure 4. <sup>b</sup> Flux estimate was derived by scaling the NMHC<sub>*i*</sub>/methane ratio to the  $55 \times 10^3$  kg h<sup>-1</sup> flux for Feb 3, 2012, reported by Karion et al.<sup>21</sup> and extrapolating to a full year assuming a constant flux. <sup>c</sup> Not individually quantified NMHCs were estimated to be ~15% of the sum of the listed species. See the Supporting Information, note 1.

Information for details of the standards). Our laboratory GC calibration scale has been cross-referenced against other national and international laboratories, including two audits by the World Calibration Centre for VOC,<sup>11</sup> with VOC results meeting all quality objectives of the WMO-GAW.<sup>10</sup> Increasing volume sample collections were conducted to affirm linearity of

the NMHC quantification beyond the nominal calibration gas scale. Uncertainty in the VOC measurements is estimated at ~5%, resulting from an on average 2–5% measurement precision error and ~2% uncertainty in the standard accuracy.

Regional NMHC background mole fractions were determined by extracting data for 40°N latitude from the representation of the global NMHC distribution (see the example for ethane in the Supporting Information, Figure 2) from data collected in the Global VOC Monitoring Program.<sup>12</sup> From the 40°N seasonal cycle the data for the period of the experiment from 2006 to 2010 were averaged for comparison with the UBWOS results. Correlations between NMHCs and methane were determined by combining the 2012 and 2013 surface data and determining the regression line slope using a bisquare-weighted least-squares analysis.

## RESULTS AND DISCUSSION

The conditions in 2012 and 2013 were markedly different. The 2012 winter was unseasonably warm with no snow-cover. Under these conditions, daytime surface heating caused mixed boundary layer conditions breaking up nighttime surface inversions and diluting accumulated surface emissions. The 2013 winter had lower temperatures and persistent snow-cover, causing prolonged temperature inversion “cold-pool” events and accumulation of surface emissions over multiple days. More in depth discussion of boundary layer mixing will be presented in forthcoming publications.

Time series data and composite diurnal cycles for surface (2 m) ozone and methane measurements from the 2012 and 2013 studies are presented in Figure 2 (see the Supporting Information, Figure 3, for the composite diurnal ethane

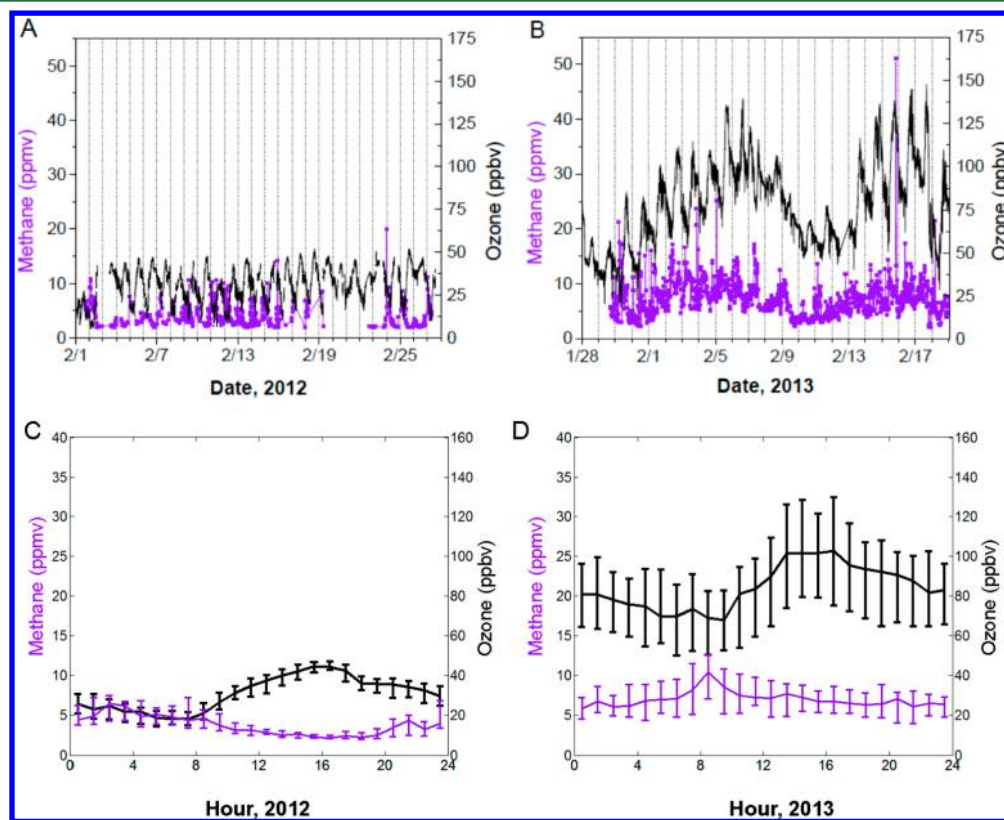


**Figure 2.** Time series data (top) and composite diurnal cycle of average hourly data (bottom) of methane and ozone measured at 2 m above the ground during the 2012 and 2013 experiments, with error bars indicating the 25–75 percentile range of the data in each hour bin.

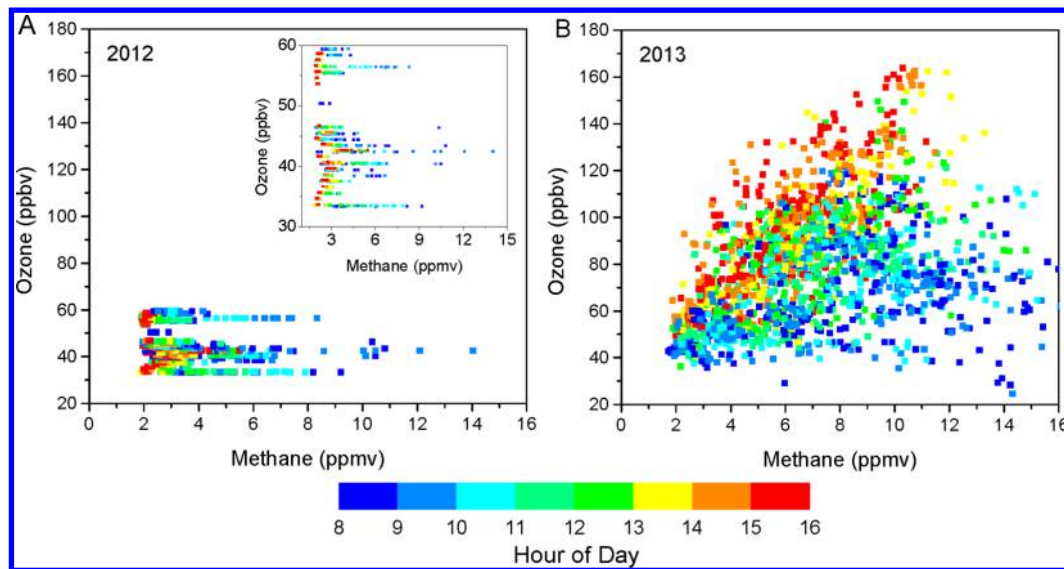


**Figure 3.** Relationship between ozone and methane during 2012 and 2013. Data shown are from 8 am – 4 pm only, with data points colored by the time of measurement. The insert in panel A shows an enlargement for the 2012 30–60 ppbv ozone data.

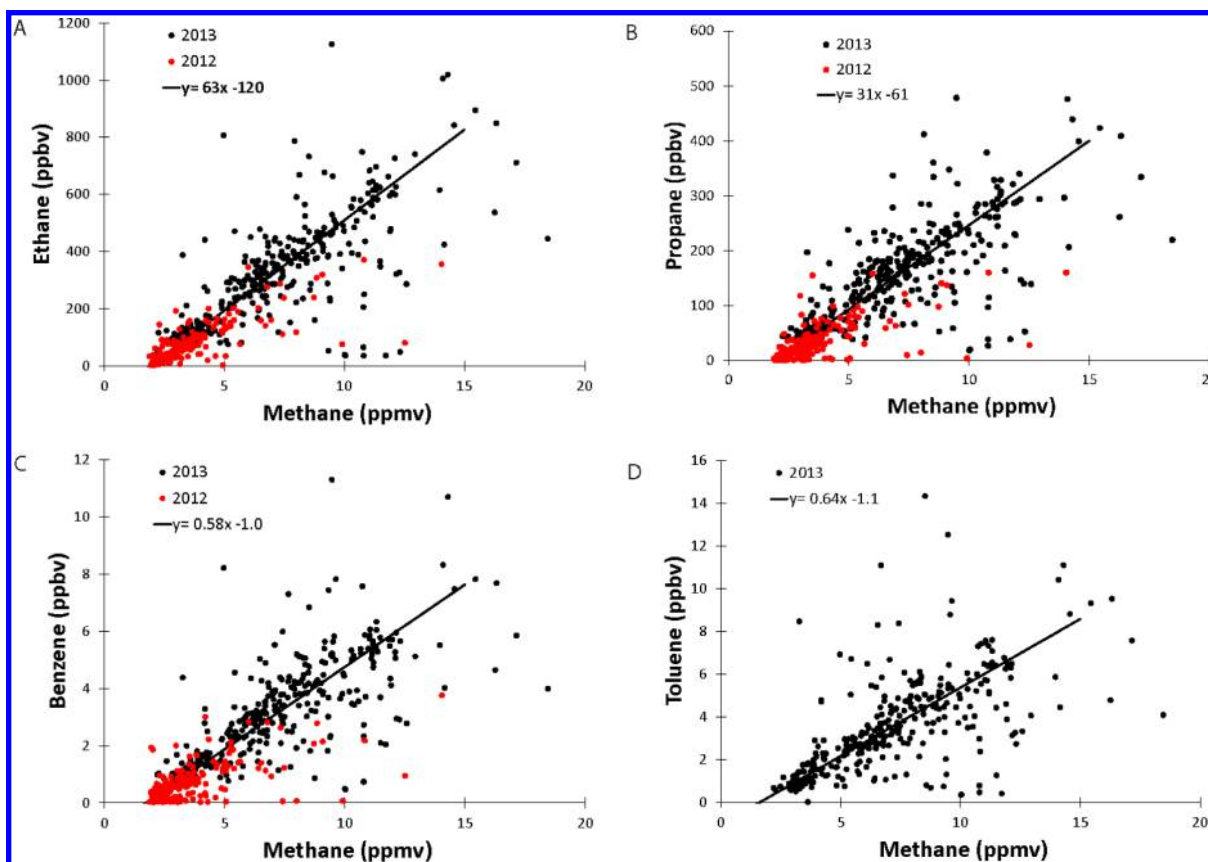


**Figure 4.** NMHC (ethane, propane, benzene, toluene) to methane relationship in all of the 2012 and 2013 surface data (for toluene 2013 only). The included regression line is the best fit through the combined 2012 and 2013 data, with regression slope results shown in the legend.

results). In 2012, the mole fractions of both gases were highly variable, with methane showing highest values during nighttime, frequently building up to  $\sim 10$  ppmv at night, and dropping to values in the 1.9–2.0 ppmv range during the middle of the day. These nighttime methane levels are exceptionally high, largely exceeding the  $\sim 1.9$  ppmv methane background mole fraction.<sup>13</sup> Similar enhancements in methane mole fractions have previously been reported from other oil and

gas producing areas.<sup>14,15</sup> Ozone dropped to minimum levels of  $\sim 20$  ppbv at night and showed rapid growth to  $\sim 40$ – $50$  ppbv after sunrise, reaching maximum values in the early afternoon. In 2013, both methane and ozone ambient air mole fractions were significantly higher than in 2012. Two distinct periods are evident during which ambient ozone exhibited strong build-up over 5–9 days (Jan 30–Feb 7, Feb 13–17) and reaching up to nearly 150 ppbv, coinciding with persistent surface temperature

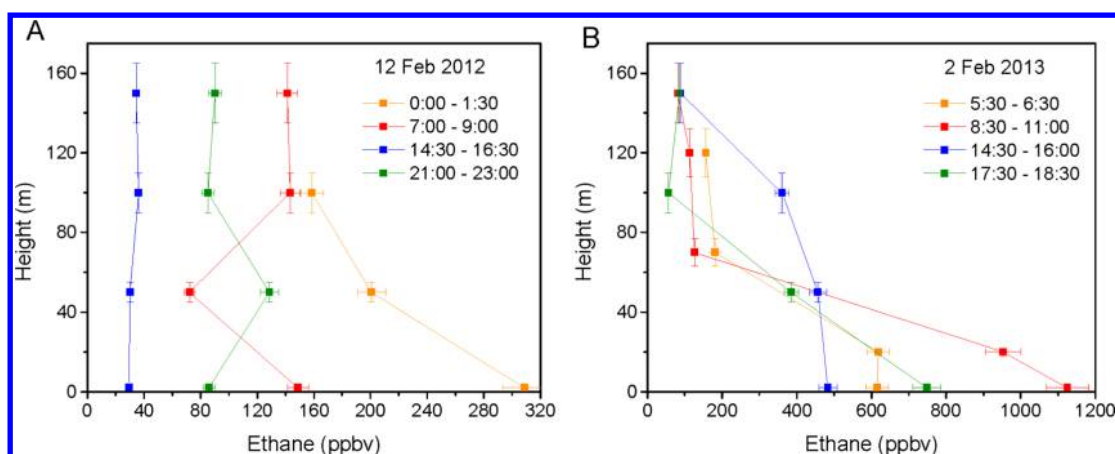


**Figure 5.** Examples of diurnal evolution of ethane vertical profiles on Feb 12, 2012 (left) and Feb 2, 2013 (right). Sampling intervals indicate the period during which individual profiles were collected, with individual height samples collected over 6 min (in situ GC) sampling time consecutively during that period with 30 min intervals in between. (Note the ~4-fold difference in the x-axis scale between both graphs; error bars indicate the 1 $\sigma$  uncertainty in the measurement.)

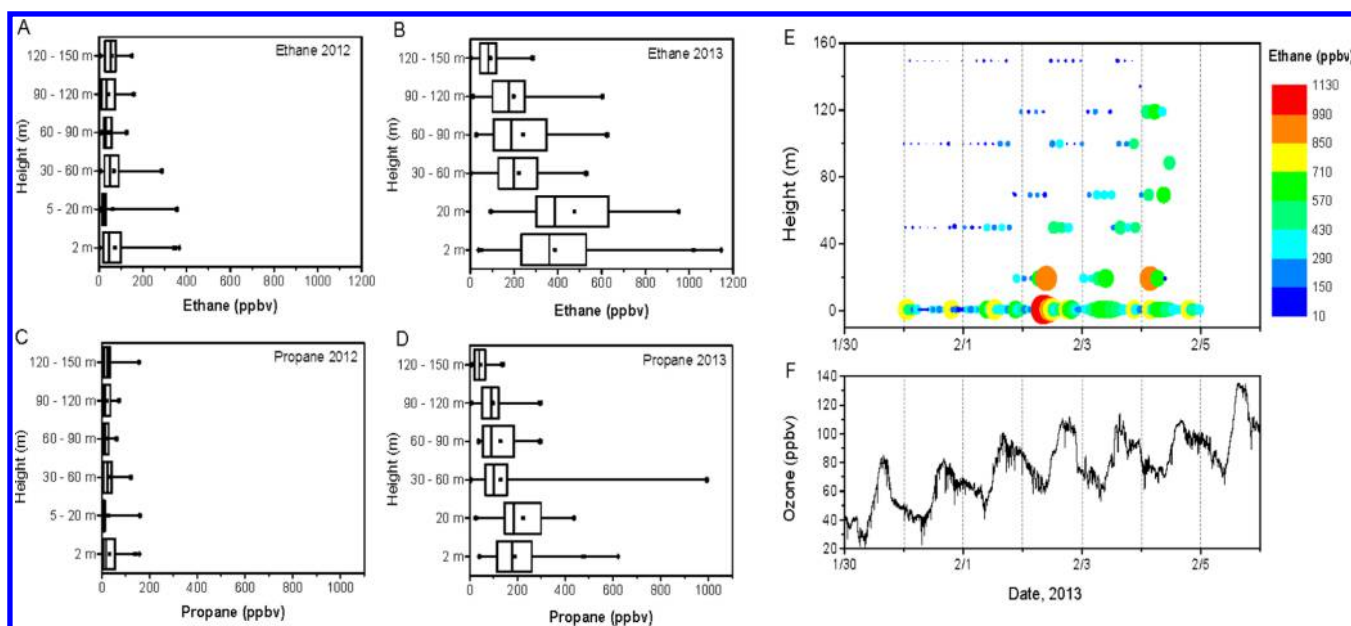


**Figure 6.** Box-whisker plots showing the vertical distribution of ethane and propane during both experiments (left) from all available tethered balloon data, with the 2-m data filtered for times when the balloon was up. Boxes outline the 25–75 percentile of the data, the vertical line inside the box the median, the dots the mean, and the whiskers the minimum and maximum values. The right panel shows the buildup of ethane with height and time during the Jan 31–Feb 9, 2013, ozone pollution event, with the circle size being proportional to the measured ethane mole fraction, and ozone measured from the 2-m tower inlet.

inversion events. Methane, likewise, showed accumulation in the surface layer during the inversion events; methane remained elevated during day and night and regularly exceeded 10 ppmv. In 2013, 1-h ozone levels peaked above 140 ppbv on 3 days during the campaign. The 8-h 75 ppbv NAAQS was exceeded during 340 h, representing 56% of the time during the 2013 experiment. The intermittent drop in both methane and ozone during Feb 9–12, 2013, was caused by passage of a low-pressure system that broke up the capping inversion and brought in air from the west of the Uintah Basin over the Wasatch Range. A noteworthy feature in the 2013 data is the similarity in the multiday timing of the buildup of methane and ozone. Concentration changes of VOC mirrored those of methane (see discussions below); this relationship suggests a tight coupling between emissions and accumulation of VOC

with ozone production. The 2013 data, much in contrast to 2012, show correlation between ozone and methane (Figure 3) with the slope of the regression increasing with time of day; afternoon, i.e., 12–4 pm data only, yield an  $R^2 = 0.5$ . Ozone continued to increase for another 3–5 days after methane reached constant levels (Figure 2b). This feature suggests continuing ozone buildup after its precursors leveled out at steady state concentrations.

Figure 4 shows the results for four NMHC/methane correlations in the 2012 and 2013 surface measurements. Similar to methane, NMHC levels were higher during 2013 in comparison to the prior snow-free year, but both years show similar correlation behavior. The data in Table 1 summarize the slope results for these analyses. Included are results for the two aromatic compounds benzene and toluene, which have been

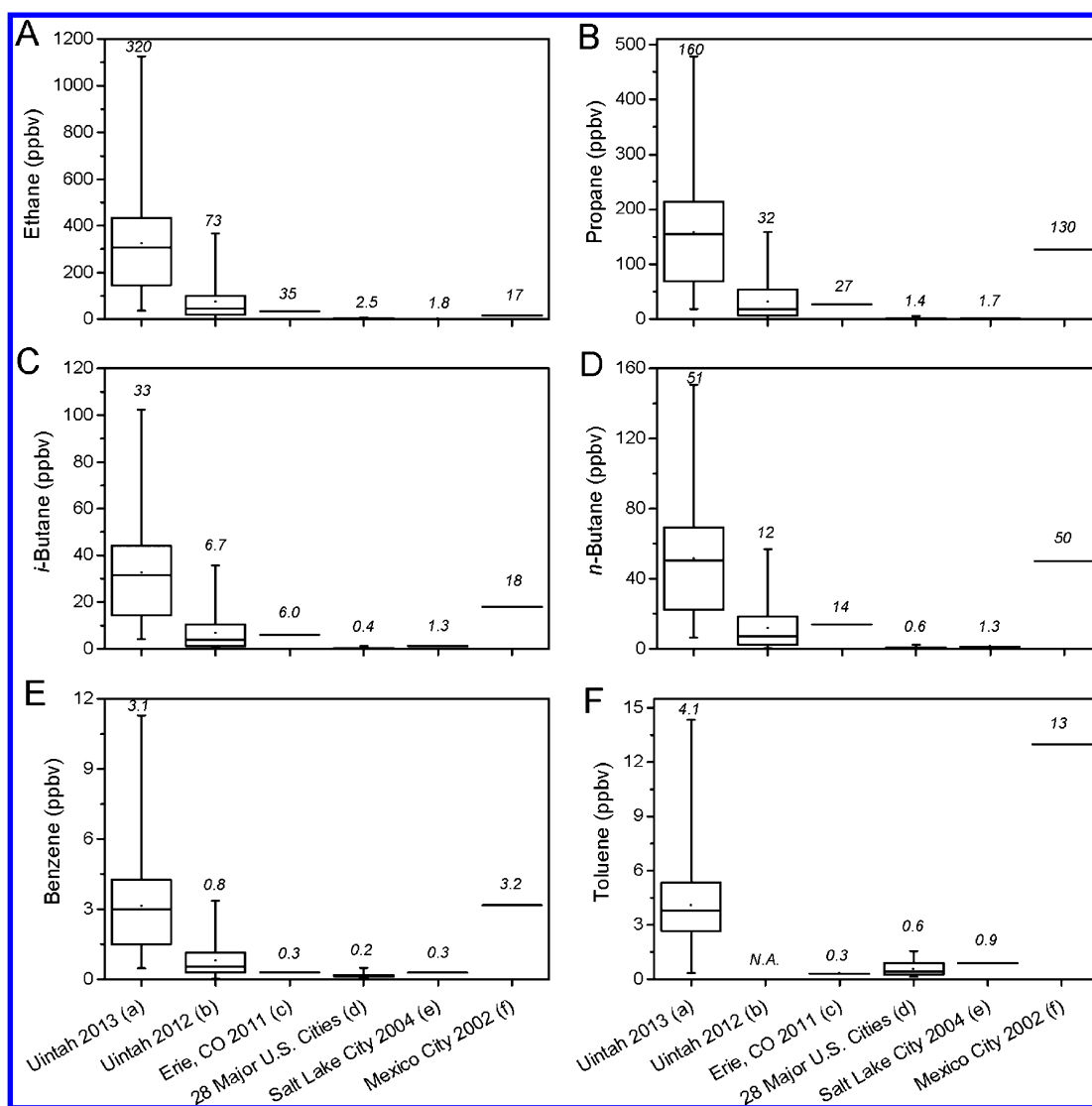


**Figure 7.** Statistical box-whisker plot comparison of the 2012 and 2013 surface (2 m) observations of ethane, propane, isobutane, *n*-butane, benzene, and toluene during the UBWOS with other selected published data. Boxes outline the 25–75 percentile of the data, the horizontal line inside the box the median, dots the mean, and the whiskers the minimum and maximum values. The dot inside the box shows the mean value. Values above the whisker bars give the mean value for the study. Explanation of the letter code for the listed studies:

<sup>a</sup>Statistics of 330 individual NMHC measurements. <sup>b</sup>Statistics of 136 individual NMHC measurements. <sup>c</sup>Mean value of 554 individual measurements, February 18–March 7, 2011.<sup>20</sup> <sup>d</sup>Statistics of 28 mean values for 28 major U.S. cities from canister samples collected during August–September between 1999 and 2005.<sup>30</sup> <sup>e</sup>Mean value of 19 individual canister samples, August–September 2004.<sup>30</sup> <sup>f</sup>Mean value of a subset of 230 canister samples collected during morning hours at four urban sites in Mexico City, Feb. 2002 and April–May 2003.<sup>31</sup>

regulated by the EPA for over 30 years, as these, besides contributing to ozone production, are known to cause direct health impacts from short and long-term exposure, with benzene being a human carcinogen.<sup>16,17</sup> Ambient air mole fractions regularly exceeded the 1.4 ppbv chronic effects screening level health threshold<sup>18</sup> for benzene (22 out of 136 measurements in 2012; 254 out of 329 measurements in 2013).

Analogous to methane, during the 2013 campaign, NMHCs built up to higher levels than in 2012 and remained elevated throughout the day and night during the majority of the campaign. NMHC atmospheric mole fractions during most times were highest near the surface and decreased with height. Diurnal NMHC vertical profiles are shown in Figure 5, and the statistical analysis of all available ethane and propane tethered balloon data is shown in Figure 6. These graphs illustrate that

in 2012 NMHCs were elevated throughout the lowest 160 m of the atmosphere, with highest levels at the surface. Concentrations built up throughout the night but dropped to lower levels during daytime hours due to the breakup of the surface inversion and mixing of cleaner air from aloft. In 2013, NMHC were even more elevated throughout the lowest 160 m of the atmosphere (note the different *x*-axis scales of the Figure 5 graphs), with again the overall highest mole fractions observed nearest to the surface. In contrast to the preceding year, in 2013, elevated surface concentrations were sustained throughout the day due to the lower degree of vertical mixing. NMHC vertical gradients with enhanced NMHC concentrations near the surface were also seen in the vertical tower gradient data set in a recent study conducted in Erie, on the western edge of the Denver–Julesburg Basin oil and gas area in Weld County,

CO;<sup>19</sup> however, absolute levels of light NMHC alkanes in the 2013 Uintah data are on the order of one magnitude higher. The right panel of Figure 6 shows that ethane built up over time and with height and that ozone buildup at the surface coincided with the increase in the ethane mole fraction. These vertical profile data are a clear indicator of the nearby surface source of NMHC emissions and strongly suggest a role of NMHC in the development of ozone pollution events.

In Figure 7, we compare the statistical distribution of the UBWOS NMHC surface measurements in 2012 and 2013 with selected recently published data from Erie; data from Salt Lake City, the one major city ~220 km upwind of the Uintah Basin; a comprehensive set of measurements from 28 US urban sites; as well as available data from Mexico City, considered one of the most polluted urban atmospheres. Note that due to the seasonal cycle of atmospheric NMHCs and long-term trends seen in urban areas, these data sets from different years and seasons can only facilitate a relatively rough comparison, which however, is useful to gauge the order of magnitude of the observed ambient NMHC mole fractions. The 2013 NMHC UBWOS light alkane data are the highest of all reported values, followed by the 2012 data set. For both years, the Uintah Basin measurements are on the order of 10–100 times higher than average ambient air mole fractions reported from the largest US cities. Uintah Basin light NMHC values are on the same order, or exceed (i.e., ethane), those for Mexico City. Interestingly, the Erie, CO, data<sup>20</sup> included in these graphs show a similar tendency of highly elevated ambient air NMHCs and are comparable to the 2012 Uintah County data. Additional measurements from the Colorado Front Range<sup>14</sup> provide further support for these highly elevated NMHC ambient air concentrations. Values measured in Salt Lake City were much lower than at the study site, by ~2 orders of magnitude for the light alkanes. This difference is much higher than what could be explained by seasonal cycles or NMHC trends (given that the reference data were collected during early fall and 8–9 years earlier). Consequently, this comparison provides a convincing argument that outflow from the state capital (which during the 2013 study period had westerly winds, and thus was upwind of the Uintah Basin ~30% of the time (see the Supporting Information, Figure S4)) is not a predominant source to the elevated Uintah Basin NMHC values.

Measurements from the NOAA/INSTAAR Global VOC Monitoring Network<sup>9</sup> allow the approximate seasonal and regional background levels of these NMHCs at the location of the study site to be defined if there were no immediate emission sources (see the Supporting Information for method description). Mean UBWOS values for ethane were 41 times (2012) and 179 times (2013) greater than background levels. The corresponding values for propane, iso-butane, *n*-butane, iso-pentane, and *n*-pentane were 42/205 (2012/2013), 49/236, 50/213, 54/220, and 83/5333, respectively (Table 2). These enhancement ratios increase with increasing molecular size, due to decreasing NMHC lifetime, resulting in lower background air concentrations and higher UBWOS/background molar ratios. This feature is a clear indication of the relatively low degree of atmospheric processing, i.e., “freshness”, of the emissions.

During UBWOS 2012, Karion et al.<sup>21</sup> used data from light aircraft measurements and a mass balance approach to estimate the methane flux for the Uintah Basin oil and gas fields. Their estimated flux of  $55 \pm 15 \times 10^3 \text{ kg h}^{-1}$  for February 3, 2012, can be used to scale up our NMHC observations for a first-

**Table 2. Comparison of UBWOS 2012 and 2013 NMHC Surface Data Results with the Estimated NMHC Regional Atmospheric Background Mole Fractions**

compound	Uintah 2012 ( <i>n</i> = 233) min – max avg (std dev) (ppbv)	Uintah 2013 ( <i>n</i> = 327) min – max average (std dev) (ppbv)	regional background 40°N, Jan 20–Feb 20 (ppbv)	enhancement factor: Uintah 2012/2013 vs background
ethane	2.04–367 74 (79)	36–1125 323 (196)	1.8	41/179
propane	1.07–158 33 (35)	19–478 158 (93)	0.77	42/205
iso-butane	0.19–36 6.8 (7.6)	4.2–102 33 (20)	0.14	49/236
<i>n</i> -butane	0.37–57 12 (13)	6.3–151 51 (30)	0.24	50/213
iso-pentane	0.11–29 5.5 (6.3)	0.98–69 22 (14)	0.10	54/220
<i>n</i> -pentane	0.098–29 5.0 (5.8)	2.4–60 20 (11)	0.06	83/333
<i>n</i> -hexane	0.047–14 2.1 (2.3)	1.2–2.5 11 (6.5)	n.a.	n.a.

order estimate of the magnitude of the NMHC flux. Note that this estimate relies on a number of simplifying assumptions, such as basin-wide constant NMHC<sub>*i*</sub>/methane ratios and constant emissions throughout the year. For this calculation, we use the individual and total NMHC/methane ratios listed in Table 1 and scale these fluxes to a year. These calculations show that fugitive annual emissions for the compounds quantified here range from 1.6–65 × 10<sup>6</sup> kg yr<sup>-1</sup>. The summation of these individual species, plus an estimated 15% for not individually quantified NMHCs (see the Supporting Information, note 1), yields a total NMHC flux estimate of (194 ± 56) × 10<sup>6</sup> kg yr<sup>-1</sup> (Supporting Information, note 2, for the uncertainty estimation), with the uncertainty estimate not considering the uncertainty in the assumptions noted above. The mass equivalent of the annual flux is approximately equivalent to 1.4 million barrels of crude oil, a ~US\$140 million value (Supporting Information, note 3). This flux can also be scaled to automobile emissions; however, it needs to be noted that this is a mass flux comparison only, which does not consider the different reactivity and toxicity of the oil and gas versus automobile emissions. VOC emissions of the current automobile fleet are on the order of 100 mg km<sup>-1</sup>.<sup>22</sup> Consequently, the fugitive NMHC mass flux from the Uintah Basin is equivalent to the VOC emissions resulting from driving a distance of 1.9 × 10<sup>12</sup> km; or, at an annual per vehicle average driving distance of 20,000 km, equivalent to the annual VOC emissions from ~100 million automobiles (Supporting Information, note 4).

Interestingly, our flux estimates for Uintah County are of similar magnitude as recent reports for the Weld County oil and gas development region. There, propane was estimated to have an annual flux of (28.5–46.3) × 10<sup>6</sup> kg yr<sup>-1</sup>, and 40 × 10<sup>6</sup> kg yr<sup>-1</sup> as calculated by Petron et al.<sup>14</sup> and Swarthout et al.,<sup>19</sup> respectively, compared to our Uintah Basin result of 41 × 10<sup>6</sup> kg yr<sup>-1</sup>. For benzene, our result of 1.6 × 10<sup>6</sup> kg yr<sup>-1</sup> is somewhat higher compared to the (0.6–1.1) × 10<sup>6</sup> kg yr<sup>-1</sup><sup>14</sup> and 0.57 × 10<sup>6</sup> kg yr<sup>-1</sup><sup>19</sup> Weld County estimates.

Karion et al. estimated the fugitive methane flux to be 6.2–11.7% of the hourly natural gas production in Uintah County. Scaling our NMHC/methane mass ratio of 0.36 to this result

yields a fugitive total NMHC flux of 2.2–4.2% of the natural gas production during the encountered conditions. Combining methane and NMHC yields a total hydrocarbon/natural gas production loss rate of 8.4–15.9%. It should be noted that because NMHCs have significantly shorter atmospheric lifetimes than methane, atmospheric NMHC/methane ratios will be lower than emission ratios, with the ratio increasing with the aging of the air and the rate of the increase increasing with molecule size. This effect will cause a negative bias in these flux estimates, causing our NMHC results to likely be lower range estimates, and actual fluxes to possibly be higher than our reported findings.

The 2013 observations from the Uintah Basin oil and gas development area are, to the best of our knowledge, among the highest ever reported mole fractions of alkane NMHCs in ambient air; mole fractions for the aromatic compounds reach or exceed those reported from the most heavily polluted inner cities. This is a remarkable finding, as the study region is a remote, rural Bureau of Land Management (BLM) area far distant from any major urban and industrial regions, which hitherto have been considered the primary emission regions for photochemical pollutants. Atmospheric NMHC levels measured in the Uintah Basin exceed results from a series of other recently published studies that demonstrated highly elevated ambient air VOC levels in oil and gas operation areas.<sup>14,19,20,23,24</sup> The cold-pool events in 2013 allowed for the accumulation of ozone precursor compounds for several days within the shallow inversion layer, leading to much enhanced pollutant levels compared with 2012. The higher albedo of the snow-covered ground in 2013 additionally led to enhanced photochemical reaction rates and higher production rates of ozone. The tight relationships between NMHCs and methane, and between ozone and methane, are a clear indication for the high ozone production resulting from emissions associated with the oil and gas extraction. These findings also support recent modeling work that investigated and postulated ozone production from oil and gas emissions<sup>25–27</sup> including the recent publication by Edwards et al.,<sup>25</sup> which utilized the UBWOS 2012 data for assessing ozone production under the conditions encountered at the Horse Pool site. These simulations, incorporating effects of snow cover and a 2-fold enhancement of VOC and radical precursors during cool pool event inversion conditions, modeled an approximate doubling of ozone production rates (i.e., from 16 to 34.6 ppbv day<sup>-1</sup>) compared to snow-free conditions. Our 2012 versus 2013 NMHC data comparison (Table 2) points toward a 4-fold increase in ambient NMHC mole fractions under snow cover conditions. Given that the photochemistry in the Uintah Basin appears to be highly sensitive to VOC,<sup>25</sup> these findings suggest higher ozone production rates than those that were modeled.<sup>25</sup> These elevated VOC levels exert health impacts through two different routes, i.e., by exceeding chronic health thresholds for long-term exposure (benzene) and by their role in contributing to ozone production resulting in exceedances of the ozone NAAQS. Oil and gas operations are increasingly moving into residential areas. Current setbacks in Colorado are ~150 m, which is less than the distance between the closest operating wells and the Horse Pool experiment site, which raises concern regarding the long-term exposure of citizens residing nearby oil and gas wells and emphasizes the importance for monitoring and assessing air quality and health impacts from oil and natural gas operations.<sup>28,29</sup>

## ■ ASSOCIATED CONTENT

### 📄 Supporting Information

Illustration of the experimental setup for the tethered balloon vertical profiling experiment, graph showing global latitudinal and seasonal distribution of ethane from the INSTAAR-NOAA/GMD global VOC monitoring program and the ethane time series extracted for 40°N, graph with the composite diurnal cycle of ethane during 2012 and 2013, and data analysis and processing details. This information is available free of charge via the Internet at <http://pubs.acs.org/>.

## ■ AUTHOR INFORMATION

### Corresponding Author

\*Tel: 001 303 492-2509. Fax: 001 303 492-6233. E-mail: [detlev.helmig@colorado.edu](mailto:detlev.helmig@colorado.edu).

### Notes

The authors declare no competing financial interest.

## ■ ACKNOWLEDGMENTS

Lee Mauldin, Abigale Curtis, Jason Sauer, Brie van Dam, and Jorrel Torres helped with the field work. Brian Seok assisted with data acquisition programming. Funding and the methane/THC monitor were provided by the State of Utah Department of Environmental Quality. We thank our colleagues from NOAA CSD and GMD for help with the field project. Sam Oltmans, NOAA GMD, provided the map used in Figure 1.

## ■ REFERENCES

- (1) Chameides, W. L.; Fehsenfeld, F.; Rodgers, M. O.; Cardelino, C.; Martinez, J.; Parrish, D.; Lonneman, W.; Lawson, D. R.; Rasmussen, R. A.; Zimmerman, P.; Greenberg, J.; Middleton, P.; Wang, T. Ozone precursor relationships in the ambient atmosphere. *J. Geophys. Res.-Atmos.* **1992**, *97* (D5), 6037–6055.
- (2) Bell, M. L.; Dominici, F.; Samet, J. M. Meta-analysis of ozone and mortality. *Epidemiology* **2005**, *16* (5), S35–S35.
- (3) Schnell, R. C.; Oltmans, S. J.; Neely, R. R.; Endres, M. S.; Molenaar, J. V.; White, A. B. Rapid photochemical production of ozone at high concentrations in a rural site during winter. *Nature Geoscience* **2009**, *2* (2), 120–122.
- (4) Rappenglueck, B.; Ackermann, L.; Alvarez, S.; Golovko, J.; Buhr, M.; Field, R.; Slotis, J.; Montague, D. C.; Hauze, B.; Adamson, S.; Risch, D.; Wilkerson, G.; Bush, D.; Stoekenius, T.; Keslar, C. Strong wintertime ozone events in the Upper Green River Basin, Wyoming. *Atmos. Chem. Phys. Discuss.* **2013**, *13*, 17953–18005.
- (5) Utah, Final Report. 2012 Uintah Basin Winter Ozone & Air Quality Study. Department of Environmental Quality, 2012, 1–281. [http://rd.usu.edu/files/uploads/ubos\\_2011-12\\_final\\_report.pdf](http://rd.usu.edu/files/uploads/ubos_2011-12_final_report.pdf) (accessed March 2014).
- (6) Oltmans, S.; Schnell, R. C.; Johnson, B.; Petron, G.; Mefford, T.; Neely, R. N. I. Anatomy of wintertime ozone associated with oil and natural gas extraction activity in Wyoming and Utah. *Elementa* **2014**, DOI: 10.12952/journal.elementa.000024.
- (7) South Coast Air Quality Management District (S. C. A. Q. M.) <http://www.aqmd.gov/smog/o3trend.html> (accessed March 2014).
- (8) Tanner, D.; Helmig, D.; Hueber, J.; Goldan, P. Gas chromatography system for the automated, unattended, and cryogen-free monitoring of C2 to C6 non-methane hydrocarbons in the remote troposphere. *J. Chromatogr. A* **2006**, *1111* (1), 76–88.
- (9) Helmig, D.; Bottenheim, J.; Galbally, I. E.; Lewis, A.; Milton, M. J. T.; Penkett, S.; Plass-Duelmer, C.; Reimann, S.; Tans, P.; Theil, S. Volatile Organic Compounds in the Global Atmosphere. *Eos Trans. AGU* **2009**, *90*, (52).
- (10) WMO. A WMO/GAW Expert Workshop on Global Long-Term Measurements of Volatile Organic Compounds (VOCs). WMO



Report No. 171, 2007, Geneva, Switzerland, 30 Jan–1 Feb 2006, 36 pp.

(11) World Calibration Centre for Volatile Organic Compounds (WCC-VOC). Karlsruhe Institute of Technology. <http://imk-ifu.fzk.de/wcc-voc/> (accessed March 2014).

(12) Global Atmospheric Volatile Organic Compound Monitoring Program. [http://instaar.colorado.edu/arl/Global\\_VOC.html](http://instaar.colorado.edu/arl/Global_VOC.html) (accessed March 2014).

(13) Dlugokencky, E. J.; Nisbet, E. G.; Fisher, R.; Lowry, D. Global atmospheric methane: budget, changes and dangers. *Philos. Trans. R. Soc. A-Math. Phys. Eng. Sci.* **2011**, *369* (1943), 2058–2072.

(14) Pétron, G.; Frost, G.; Miller, B. R.; Hirsch, A. L.; Montzka, S. A.; Karion, A.; Trainer, M.; Sweeney, C.; Andrews, A. E.; Miller, L.; Kofler, J.; Bar-Ilan, A.; Dlugokencky, E. J.; Patrick, L.; Moore, C. T.; Ryerson, T. B.; Siso, C.; Kolodzey, W.; Lang, P. M.; Conway, T.; Novelli, P.; Masarie, K.; Hall, B.; Guenther, D.; Kitzis, D.; Miller, J.; Welsh, D.; Wolfe, D.; Neff, W.; Tans, P. Hydrocarbon emissions characterization in the Colorado Front Range: A pilot study. *J. Geophys. Res.-Atmos.* **2012**, *117*, 1–19.

(15) Tollefson, J. Air sampling reveals high emissions from gas field. *Nature* **2012**, *482* (7384), 139–140.

(16) Wallace, L. Environmental exposure to benzene: An update. *Environ. Health Perspect.* **1996**, *104*, 1129–1136.

(17) Suh, H. H.; Bahadori, T.; Vallarino, J.; Spengler, J. D. Criteria air pollutants and toxic air pollutants. *Environ. Health Perspect.* **2000**, *108*, 625–633.

(18) TCEQ Guidelines to Develop Toxicity Factors. RG-442 Revised DRAFT, 2012. [http://www.tceq.state.tx.us/toxicology/esl/list\\_main.htm](http://www.tceq.state.tx.us/toxicology/esl/list_main.htm) (accessed January 2014).

(19) Swarthout, R. F.; Russo, R. S.; Zhou, Y.; Hart, A. H.; Sive, B. C. Volatile organic compound distributions during the NACHTT campaign at the Boulder Atmospheric Observatory: Influence of urban and natural gas sources. *J. Geophys. Res.-Atmos.* **2013**, *118* (18), 10614–10637.

(20) Gilman, J. B.; Lerner, B. M.; Kuster, W. C.; de Gouw, J. A. Source signature of volatile organic compounds from oil and natural gas operations in northeastern Colorado. *Environ. Sci. Technol.* **2013**, *47* (3), 1297–1305.

(21) Karion, A.; Sweeney, C.; Petron, G.; Frost, G.; Hardesty, M.; Kofler, J.; Miller, B. R.; Newberger, T.; Wolter, S.; Banta, R.; Brewer, A.; Dlugokencky, E. J.; Lang, P.; Montzka, S. A.; Schnell, R. C.; Tans, P.; Trainer, M.; Zomora, R.; Conley, S. Methane emissions estimate from airborne measurements over a western United States natural gas field. *Geophys. Res. Lett.* **2013**, *40*, 1–5.

(22) Ho, K. F.; Lee, S. C.; Ho, W. K.; Blake, D. R.; Cheng, Y.; Li, Y. S.; Ho, S. S. H.; Fung, K.; Louie, P. K. K.; Park, D. Vehicular emission of volatile organic compounds (VOCs) from a tunnel study in Hong Kong. *Atmos. Chem. Phys.* **2009**, *9* (19), 7491–7504.

(23) Katzenstein, A. S.; Doezema, L. A.; Simpson, I. J.; Balke, D. R.; Rowland, F. S. Extensive regional atmospheric hydrocarbon pollution in the southwestern United States. *Proc. Natl. Acad. Sci. U.S.A.* **2003**, *100* (21), 11975–11979.

(24) Simpson, I. J.; Blake, N. J.; Barletta, B.; Diskin, G. S.; Fuelberg, H. E.; Gorham, K.; Huey, L. G.; Meinardi, S.; Rowland, F. S.; Vay, S. A.; Weinheimer, A. J.; Yang, M.; Blake, D. R. Characterization of trace gases measured over Alberta oil sands mining operations: 76 speciated C<sub>2</sub>-C<sub>10</sub> volatile organic compounds (VOCs), CO<sub>2</sub>, CH<sub>4</sub>, CO, NO, NO<sub>2</sub>, NO<sub>y</sub>, O<sub>3</sub> and SO<sub>2</sub>. *Atmos. Chem. Phys.* **2010**, *10* (23), 11931–11954.

(25) Edwards, P. M.; Young, C. J.; Aikin, K.; deGouw, J. A.; Dubé, W. P.; Geiger, F.; Gilman, J. B.; Helmig, D.; Holloway, J. S.; Kercher, J.; Lerner, B.; Martin, R.; McLaren, R.; Parrish, D. D.; Peischl, J.; Roberts, J. M.; Ryerson, T. B.; Thornton, J.; Warneke, C.; Williams, E. J.; Brown, S. S. Ozone photochemistry in an oil and natural gas extraction region during winter: simulations of a snow-free season in the Uintah Basin, Utah. *Atmos. Chem. Phys. Discuss.* **2013**, *13* (3), 7503–7552.

(26) Kembal-Cook, S.; Bar-Ilan, A.; Grant, J.; Parker, L.; Jung, J. G.; Santamaria, W.; Mathews, J.; Yarwood, G. Ozone impacts of natural

gas development in the Haynesville Shale. *Environ. Sci. Technol.* **2010**, *44* (24), 9357–9363.

(27) Carter, W. P. L.; Seinfeld, J. H. Winter ozone formation and VOC incremental reactivities in the Upper Green River Basin of Wyoming. *Atmos. Environ.* **2012**, *50*, 255–266.

(28) McKenzie, L. M.; Witter, R. Z.; Newman, L. S.; Adgate, J. L. Human health risk assessment of air emissions from development of unconventional natural gas resources. *Sci. Total Environ.* **2012**, *424*, 79–87.

(29) Colburn, T.; Schultz, K.; Herrick, L.; Kwiatkowski, C., An exploratory study of air quality near natural gas operations. *Hum. Ecol. Risk Assess.* **2013**, doi.org/10.1080/10807039.2012.749447.

(30) Baker, A. K.; Beyersdorf, A. J.; Doezema, L. A.; Katzenstein, A.; Meinardi, S.; Simpson, I. J.; Blake, D. R.; Rowland, F. S. Measurements of nonmethane hydrocarbons in 28 United States cities. *Atmos. Environ.* **2008**, *42* (1), 170–182.

(31) Velasco, E.; Lamb, B.; Westberg, H.; Allwine, E.; Sosa, G.; Arriaga-Colina, J. L.; Jobson, B. T.; Alexander, M. L.; Prazeller, P.; Knighton, W. B.; Rogers, T. M.; Grutter, M.; Herndon, S. C.; Kolb, C. E.; Zavala, M.; de Foy, B.; Volkamer, R.; Molina, L. T.; Molina, M. J. Distribution, magnitudes, reactivities, ratios and diurnal patterns of volatile organic compounds in the Valley of Mexico during the MCMA 2002 & 2003 field campaigns. *Atmos. Chem. Phys.* **2007**, *7*, 329–353.